Theor Appl Climatol (2016) 125:625–639
DOI 10.1007/s00704-015-1517-8

ORIGINAL PAPER

Influence of atmospheric circulation patterns on local cloud and solar variability in Bergen, Norway

Kajsa Parding[1,4] · Jan Asle Olseth[1] · Beate G. Liepert[2] · Knut-Frode Dagestad[3]

Received: 15 October 2014 / Accepted: 19 May 2015 / Published online: 20 June 2015

Abstract In a previous paper, we have shown that long-term cloud and solar observations (1965–2013) in Bergen, Norway (60.39°N, 5.33°E) are compatible with a largely cloud dominated radiative climate. Here, we explicitly address the relationship between the large scale circulation over Europe and local conditions in Bergen, identifying specific circulation shifts that have contributed to the observed cloud and solar variations. As a measure of synoptic weather patterns, we use the Grosswetterlagen (GWL), a daily classification of European weather for 1881–2013. Empirical models of cloud cover, cloud base, relative sunshine duration, and normalised global irradiance are constructed based on the GWL frequencies, extending the observational time series by more than 70 years. The GWL models successfully reproduce the observed increase in cloud cover and decrease in solar irradiance during the 1970s and 1980s. This cloud-induced dimming is traced to an increasing frequency of cyclonic and decreasing frequency of anticyclonic weather patterns over northern Europe. The changing circulation patterns in winter can be understood as a shift from the negative to the positive phase of the North Atlantic and Arctic Oscillation. A recent period of increasing solar irradiance is observed but not reproduce by the GWL models, suggesting this brightening is associated with factors other than large scale atmospheric circulation, possibly decreasing aerosol loads and local cloud shifts.

✉ Kajsa Parding
kajsa.parding@gfi.uib.no; kajsa.parding@met.no

1 University of Bergen, Bergen, Norway

2 NorthWest Research Associates, Redmond, WA, USA

3 Norwegian Meteorological Institute, Bergen, Norway

4 Present address: Norwegian Meteorological Institute, Oslo, Norway

1 Introduction

The shortwave (SW) irradiance measured at the Earth's surface varies considerably on decadal to multidecadal time scales. Studies have reported a wide spread decrease of SW irradiance from the 1950s to the 1980s, followed by increasing SW irradiance in the 1990s in many regions, including northern Europe (Stanhill and Cohen 2001; Liepert 2002; Wild et al. 2005; Russak 2009; Gilgen et al. 2009; Liley 2009). The observed decadal SW irradiance trends are commonly referred to as dimming and brightening (Wild 2012). Aerosol emissions have been implicated as a contribution factor to the dimming and brightening in many parts of the world, but natural cloud variability have also been found to play a dominant role in some regions, e.g., Alaska (Wild 2012; Chiacchio et al. 2010). The relative importance of aerosols and clouds vary depending on the meteorological conditions as well as local and long-range sources of aerosols (Wild 2012). Therefore, a local perspective can be more useful than a continental or worldwide approach when investigating the implications and root causes global dimming and brightening.

In a previous paper (Parding et al. 2014), we studied solar irradiance and cloud changes at the high latitude coastal site Bergen in Norway. Observations of clouds and SW irradiance are compatible with a largely cloud dominated radiative climate and show a significant dimming in the late 1970s and 1980s (Parding et al. 2014; Stjern et al. 2009). A recent brightening period after 1990, seen in Bergen as well as other parts of Europe, is at first glance

at odds with the local cloud cover observations. A seasonal analysis revealed a cloud cover decrease in the months of strongest brightening in Bergen, but we could not exclude the possibility of other factors also adding to the brightening, e.g., the locally observed aerosol optical depth which decreases considerably during the 1990s. In Parding et al. (2014), we suggested that the observed cloud changes in Bergen are connected to the variability of the storm frequency, which has a dominant influence on the weather conditions on the Atlantic European coastal region and northern Eurasia at large (Budikova 2012). Nevertheless, an indirect effect of aerosols acting as cloud condensation nuclei cannot be unequivocally excluded as a cause of the cloud changes based on local cloud and solar observations alone.

In this paper, we isolate the effects of atmospheric dynamics and thus directly address the connection between large scale circulation patterns and the local cloud and solar conditions in Bergen. The results presented in this paper are not representative of Europe or the whole Scandinavian region, but the method of downscaling large scale weather patterns to local meteorological conditions should be applicable to any site. As a measure of the large scale meteorological conditions, we use the Grosswetterlagen (GWL), a daily classification of European weather patterns from 1881 to 2013 which represents 29 common weather situations. Using the frequencies of the GWL, we construct empirical models of cloud and solar observations which extend the observational time series by more than 70 years back to 1881. The indirect and direct effect of aerosols on SW irradiance is assessed based on the deviation between simulated and observed time series of cloud and solar variables.

2 Data description

Bergen is situated on the west coast of Norway in a north-south oriented valley, approximately 15 km long and 300–600 m deep (Hanssen-Bauer 1967). The climate is maritime and temperate, with monthly mean temperatures ranging from 1.5 °C in January and 14.5 °C in July and on average 235 precipitation days (>0.1 mm) per year, among the highest precipitation rates in Europe (annual precipitation 2250 mm). (The climatological values are based on observations during the reference period 1961–1990 and are available from the NOAA world weather website www.worldweather.wmo.int). Cloud formation and precipitation is promoted by orographic lifting of the air along the mountains surrounding the city. The meteorological conditions in Bergen are also strongly influenced by synoptic weather patterns and storms associated with the North Atlantic storm track. The observations used in this study are from the meteorological station Florida which is located on the roof top of the Geophysical Institute, University of Bergen, in the city center.

Solar measurements have been conducted in Bergen for more than 60 years. Since 1952, the sunshine duration has been measured by a Campbell-Stokes sunshine recorder, an instrument consisting of a glass sphere that focuses the incoming solar radiation on to a paper strip (Stanhill 2003). The beam burns the paper strip when the direct shortwave irradiance exceeds a threshold (205 ± 35 Wm^{-2}).

In 1965, two pyranometers were installed to measure the global and diffuse SW irradiance, the diffuse irradiance instrument with a circular disc mounted on a rotating arm to shadow the direct irradiance. In Parding et al. (2014), we describe the calibration history of the SW irradiance measurements and estimate the uncertainty of the SW irradiance observations in Bergen. The relative uncertainty of the SW irradiance measurements is approximately 3.5, 1.6, and 1.1 % for the daily, monthly, and annually averaged time series, respectively.

A normalised SW irradiance with reduced seasonal cycle is obtained by dividing the measured global irradiance by the irradiance at the top of the atmosphere. The irradiance at the top of the atmosphere is estimated based on the time and location as described in Iqbal (1983), assuming a solar constant S_0 of 1361 Wm^{-2} (Kopp and Lean 2011). The normalised global irradiance is referred to as the atmospheric transmittance (Tr) and can be interpreted as the fraction of the extraterrestrial irradiance that is transmitted through the atmosphere to the surface of the Earth at a given time. A weaker seasonal cycle remains after normalisation due to variations of the atmospheric path length.

The sunshine duration is normalised by the maximum possible sunshine duration, i.e., the length of the period during which the sun is above the natural horizon. The relative sunshine duration is reported in units of % of the maximum day length.

Visual observations of clouds have been made every 3 h since 1957, but only the 6 hourly observations (0, 6, 12, and 18 UTC = 1, 7, 13, 19 standard local time) have been transferred to digital format for the full period of available data. For consistency, we use only the 6, 12, and 18 UTC data even in periods when additional observations are available. The 0 UTC observation is excluded because it is difficult to make precise observations of clouds in the dark of the night. The cloud observations are freely available via the Norwegian Meteorological Institute's weather and climate data website Eklima (www.eklima.no).

The cloud data are reported according to Word Meteorological Organization (WMO) standards for weather observations (WMO 2008). The observed cloud variables used in this study are the total cloud cover (NN) and the cloud base height (HL). The cloud cover, NN, is reported in oktas (eighths of the sky that are covered by clouds). The cloud

base height, HL, is reported in meters according to a fixed scale that is finer at lower levels (0, 50, 100, 200, 300, 600, 1000, 1500, 2000, and 2500 m). The reported cloud base value is the lower limit of an interval; 0 m means that the cloud base is lower than 50 and 2500 m refers to clouds with a base height of 2.5 km or higher.

3 Empirical Grosswetterlagen models

As a measure of North Atlantic and European synoptic meteorological patterns, we use the GWL, a subjective weather classification first developed by Baur et al. (1944) in the 1940s and revised by Hess and Brezkowsky in 1950–1951 (Werner and Gerstengarbe 2010). The classification has been carried out for the period 1881–2014, until 1938 based on Sea Level Pressure (SLP) observations alone and since 1939 with the additional information of 500 hPa geopotential height maps of the North Atlantic and Europe (Werner and Gerstengarbe 2010). There are 29 GWL types, characterised by the position of cyclonic and anti-cyclonic weather systems and the direction of the surface flow over central Europe. Each day from 1881 to the present day has been prescribed exactly one GWL and that GWL must persist unchanged for a minimum of 3 days. Cases that do not fit any of the GWL classes or occur less than 3 days in a row have been prescribed GWL 30 = unknown (very rare, <1 % of all days are prescribed

Table 1 Large scale weather pattern types of the Grosswetterlagen (GWL) data set, a European daily weather pattern classification

#	Abbreviation	Description
1	WA	Anticyclonic westerly
2	WZ	Cyclonic westerly
3	WS	South-shifted westerly
4	WW	Maritime westerly, block Eastern Europe
5	SWA	Anticyclonic south-westerly
6	SWZ	Cyclonic south-westerly
7	NWA	Anticyclonic north-westerly
8	NWZ	Cyclonic North-Westerly
9	HM	High over central Europe
10	BM	Zonal ridge across central Europe
11	TM	Low (cut-off) over central Europe
12	NA	Anticyclonic northerly
13	NZ	Cyclonic northerly
14	HNA	Icelandic high, ridge over central Europe
15	HNZ	Icelandic high, trough over central Europe
16	HB	High over the British Isles
17	TRM	Trough over central Europe
18	NEA	Anticyclonic north-easterly
19	NEZ	Cyclonic north-easterly
20	HFA	Scandinavian high, ridge over central Europe
21	HFZ	Scandinavian high, trough over central Europe
22	HNFA	Scandinavian-Iceland high, ridge over central Europe
23	HNFZ	Scandinavian-Iceland high, trough over central Europe
24	SEA	Anticyclonic south-easterly
25	SEZ	Cyclonic south-easterly
26	SA	Anticyclonic southerly
27	SZ	Cyclonic southerly
28	TB	Low over the British Isles
29	TRW	Trough over western Europe
30	U	Undefined

The table includes a brief description of the dominant features of the weather patterns over central Europe and the North Atlantic as well as the GWL number (#) and the abbreviations by which they are referred to in the Grosswetterlagen catalogue (Werner and Gerstengarbe 2010)

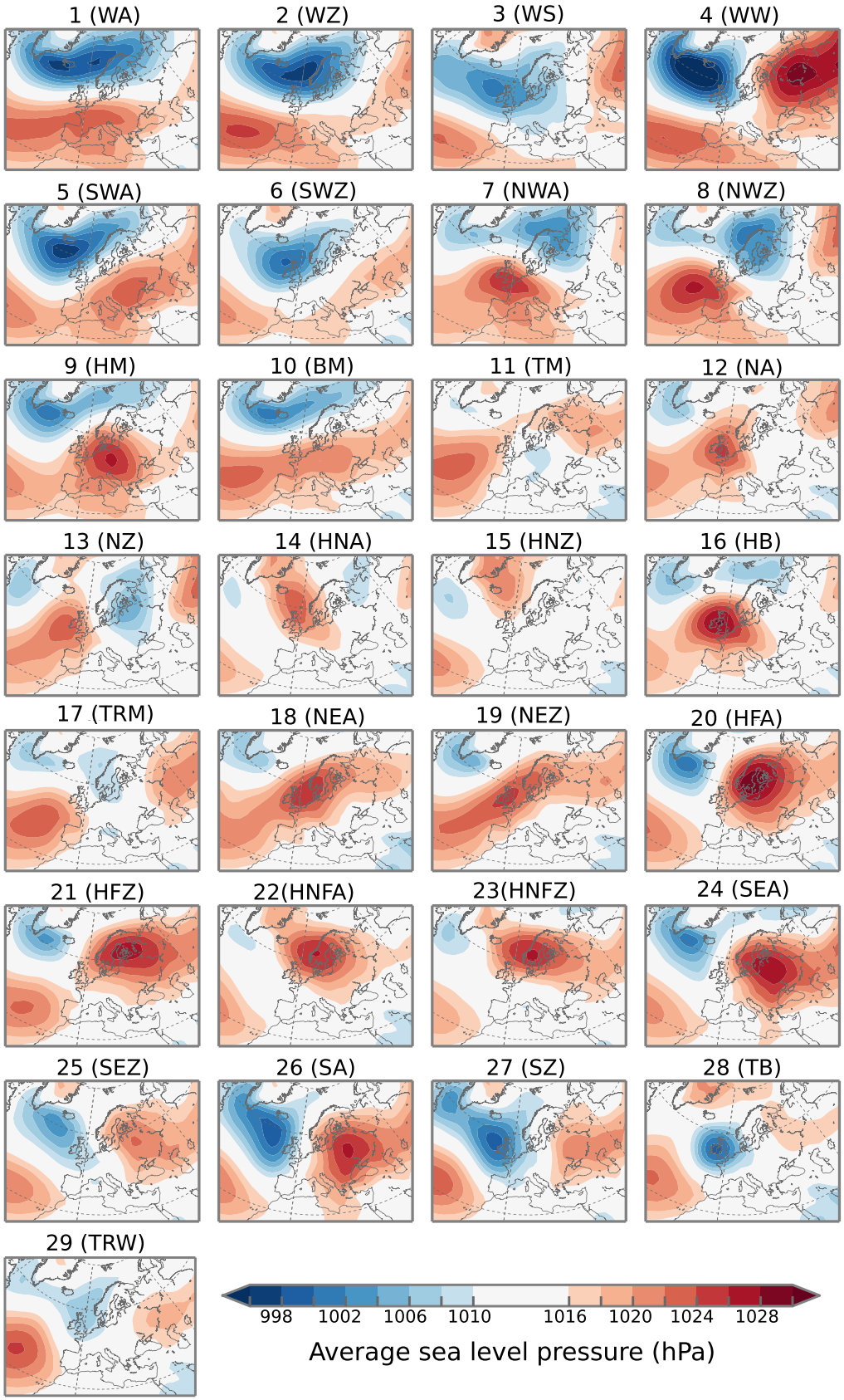

Fig. 1 Patterns of average sea level pressure (hPa) over Europe associated with the 29 Grosswetterlagen types, calculated based on daily SLP data (NCEP reanalysis 2) from 1979–2012

GWL 30). The average persistence of the GWL is approximately 5 days. The synoptic situation is obviously not constant on time scales shorter than 5 days, but the GWL capture the quasi-stationary slow changing large scale structure of the atmospheric circulation. Descriptions of the GWL types are shown in Table 1. The SLP patterns associated with each of the 29 GWL weather pattern types are displayed in Fig. 1. The SLP maps are plotted with the daily NCEP-DOE Reanalysis 2 data from 1979–2012, provided by the NOAA/OAR/ESRL PSD (Boulder, Colorado, USA) from the web site http://www.esrl.noaa.gov/psd/ (Kanamitsu et al. 2002).

Empirical models of cloud and solar observations are constructed from the GWL frequencies. The GWL models can be interpreted as the portion of the local cloud and solar variability that is associated with the large scale atmospheric circulation over the North Atlantic and Europe. The models extend the cloud and radiative observational time series from Bergen by more than 70 years back to 1881, which is the start of the GWL time series.

Equation 1 describe how an empirical GWL model, $\hat{y}(\text{year})$, is constructed based on a daily observational time series, $y(d)$, and the annual mean frequencies $f_i(\text{year})$ of the 29 GWL weather patterns.

$$\hat{y}(\text{year}) = c_0 + \sum_{i=1}^{29} c_i \cdot f_i(\text{year}) \tag{1}$$

$$c_0 = \frac{1}{N} \sum_{d=d_{\text{start}}}^{d_{\text{end}}} y(d)$$

$$c_i = \frac{1}{N_i} \sum_{d=d_{\text{start}}}^{d_{\text{end}}} \delta_{i,\text{GWL}(d)} \cdot y(d) - c_0$$

where

$$\delta_{i,GWL(d)} = \begin{cases} 1 & \text{if GWL}(d) = i \\ 0 & \text{if GWL}(d) \neq i \end{cases}$$

N = total number of daily observations

$$N_i = \sum \delta_{i,GWL(d)}$$

= total number of days classified as GWL i

The annual model described in Eq. 1 is equivalent of a daily model with the same value c_i ascribed to all days d_i that have been identified as GWL i ($i \in [1, 29]$). The coefficients c_i are the anomalies of y associated with the weather patterns GWL i during the calibration period, d_{start}–d_{end}.

The models are calibrated (i.e., coefficients are calculated) using only a portion of the available observational time series, from 1990 to 2013, so that the model output can then be tested with the remaining independent observational time series. This calibration period is chosen because all observational time series considered in this study (cloud cover, cloud base, global irradiance, and sunshine duration) are available for 1990–2013. During this period, each of the GWL occur between 42 and 1400 days (the occurrence vary between different weather patterns) which should be enough to calculate coefficients that are representative of the link between the large scale weather patterns and local conditions in Bergen. Other calibration periods of equal length have been tested with little change to the resulting GWL models. For example, there is a very high correlation ($R = 0.97$) between the standard GWL model of atmospheric transmittance and the corresponding model calibrated using data from the earlier period 1966–1989.

The coefficients describe the relation between the large scale weather patterns and the resulting solar and cloud anomalies in Bergen. A positive coefficient, $c_i > 0$, shows that the weather pattern GWL i is associated with positive anomalies of the variable y, and vice versa for negative coefficients. For example, if y is the observed cloud cover, a positive coefficient indicates that GWL i is associated with anomalously cloudy conditions and a negative coefficient that the pattern is associated with clearer than average skies. If there is no connection between the observed variable and a weather pattern GWL i, then the average of y is expected to be approximately equal for days identified as GWL i as for all days, making the coefficient c_i approximately zero. If there is no connection between the observed variable and synoptic weather patterns in general, then coefficients should all be close to zero ($c_1 \approx c_2 \approx \ldots \approx c_{29} \approx 0$), resulting in a model with very little variability and hence predictability. As we will show in the Section 4 and Figs. 2 and 3, this is not the case for the models based on cloud and solar observations from Bergen.

The strong seasonal cycle of the solar irradiance, which is related to the Earth's axial tilt and orbit more than variations of the weather patterns, can potentially interfere with the model calibration. For example, a weather pattern that is more commonly occurring in summer than in winter may obtain an unrealistically high positive coefficient which indicates that it is associated with very sunny conditions. This is technically not false, but it is not representative of the atmospheric conditions associated with the weather pattern and their influence of the SW irradiance. To avoid this problem, we normalise the global irradiance and sunshine duration as described in Section 2 and fit GWL models using the atmospheric transmittance and relative sunshine duration which have reduced seasonal cycles. The weak remaining seasonal cycle of the atmospheric transmittance, which is due to variations of the atmospheric path length, does not appear to have a serious effect on the model calibration. In Parding et al. (2014), we have shown that the clouds in Bergen have a very weak seasonality (Fig. 5 in Parding et al. 2014). Hence, the seasonality does not pose a

problem when modeling the clouds. (Note this is not always true for other sites in northern Europe.)

4 Results and discussion

4.1 Comparison of observations and the GWL models

To evaluate the performance of the empirical GWL models of cloud cover, cloud base, relative sunshine duration, and atmospheric transmittance in Bergen, the model simulations are compared to observations. If the model simulation of a time series, e.g., the cloud cover, agrees well with observations, we can assume that (1) synoptic weather patterns have a dominant influence on the variable, and (2) the extended time series from 1881 to 2013 is likely representative of past weather variability also before the cloud and solar observations became available. The results are presented as scatter plots in Fig. 2 and as time series in Fig. 3. Figure 3 also includes estimates of the magnitude and 95 %-level statistical significance of linear trends calculated for 25 year long sliding periods, shown in the lower panels of the plots and marked with orange and black dots.

The empirical GWL models reproduce the cloud and solar variability in Bergen well (Figs. 2 and 3). The correlation between model simulations and annual mean observations is high and statistically significant for all the examined weather parameters. For the cloud cover, cloud base, relative sunshine duration, and atmospheric transmittance, the Pearson's correlation coefficient is 0.79, 0.78, 0.80, and 0.82, respectively, (R values shown in Fig. 2). This indicates that the varying frequency of the synoptic weather patterns (f_i in Eq. 1) account for 60–80 % of the interannual cloud and solar variability in Bergen. The correlation coefficients are calculated based on the independent data that are not used for model calibration (shown as filled markers in the scatterplots), i.e., excluding 1990–2013. The good agreement of the independent observed and model simulated values demonstrate that the relationship between large scale weather patterns and local solar and cloud conditions in Bergen, as represented by the model coefficients (c_i in Eq. 1), is stable throughout the observational period. Nevertheless, the GWL models do not perfectly reproduce the observations. In particular, the model simulations have a smaller range than observations, the model tends to underestimate high values and overestimate the low values. This can be seen in the scatter plots (Fig. 2) as a departure of the line of best fit (dashed line) from the one-to-one line (solid line).

The time series reveal a significant change in the cloud and solar variables (Fig. 3): an increase of the cloud cover and reduction of the cloud base height during the late 1970s and 1980s. During the same period, there is a corresponding negative trend in the atmospheric transmittance and relative sunshine duration, which can be described as a solar dimming. The model simulations of cloud cover, cloud base, and relative sunshine duration follow the observations closely throughout the observational period, including the dimming period, and the estimated trends (lower panels below the time series in Fig. 3) are of approximately equal magnitude for model simulations and observations. For the cloud cover, the trends of the model time series tend to be statistically significant on a higher level than the observed trends (i.e., lower p values of the Mann Kendall trend test), most likely because the inter-annual variability is smaller for the model simulation. The close resemblance between the model simulated and observed values of cloud cover, cloud base height, relative sunshine duration, and atmospheric transmittance during the late 1970s and 80s suggest that the dimming during this period is driven by cloud changes associated with the large scale circulation patterns.

Change point analysis of the observational time series does not reveal any significant shifts or inhomogeneities in cloud cover, cloud base, relative sunshine duration, or atmospheric transmittance in Bergen (method described in Lund and Reeves 2002). However, analysis of the model simulations clearly indicates a sudden shift in 1980/1981 to more cloudy and less sunny conditions (not shown visually). The change is likely recognised as a significant change point because the model simulations are more than 70 years longer than the observational records and have a smaller inter-annual variability. Given that a concurrent change is seen in both the model simulations and the observational time series of cloud cover, cloud base, and relative sunshine duration and atmospheric transmittance, we conclude that the change point in 1980/1981 represents a regime shift in the Bergen climate and not an artificial shift due to observational issues. This example also shows the inherent difficulties of trend and change point analysis of short time series.

Although the atmospheric transmittance model reproduces the observed changes well during the dimming period of the late 1970s and 80s, it fails to reproduce a series of observed positive transmittance peaks in the 2000s which can be described as a brightening. Interestingly, the GWL model of atmospheric transmittance follows the observed transmittance more closely during the independent period ($<$1990) than during the period used to calibrate the model coefficients (1990–2013). The performance of the GWL models during the brightening period suggests that while the cloud cover and cloud base is closely related to the large scale circulation, the atmospheric transmittance is influenced by factors that are not represented by the GWL data, e.g, small scale meteorological processes or aerosol emissions. As reported in Parding et al. (2014), a cloud cover

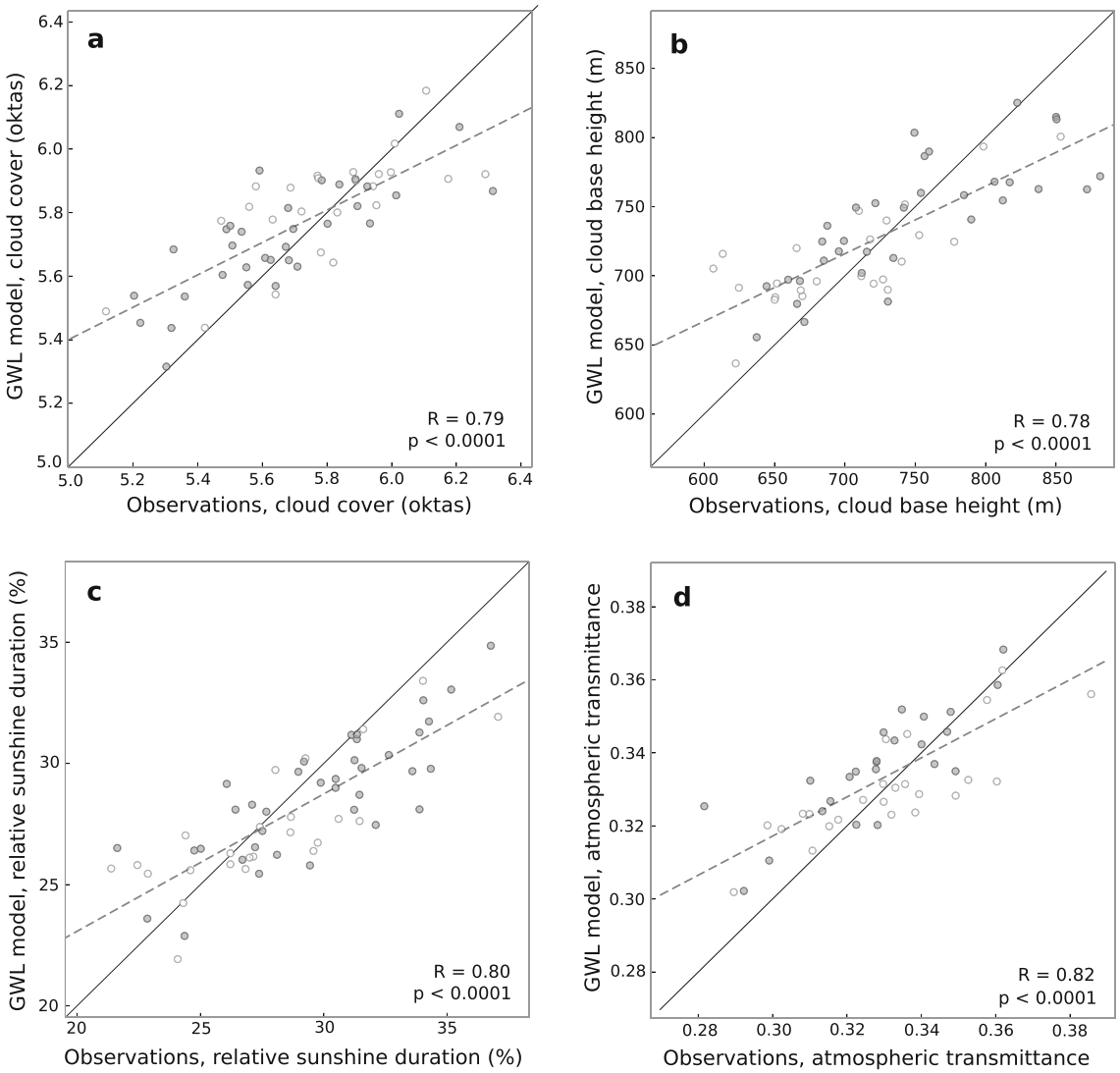

Fig. 2 Scatterplots of observational versus simulated annual mean time series of **a** cloud cover, **b** cloud base, **c** relative sunshine duration, and **d** atmospheric transmittance (normalised global irradiance) for Bergen, Norway. The empirical models are based on a daily weather pattern classification data set as described in Section 3. *Empty markers* show data for years used for model calibration (1990–2013) and filled markers show independent observations (<1990). The plots also include a reference 1:1 line (*solid line*) and a linear regression (*dashed line*). The correlation coefficient (R) of observed and modeled values and the p-value of the correlation is shown in the lower right corner of each plots. The correlation R is calculated based on the independent observations before 1990. The p is a measure of the probability with which the null hypothesis of no correlation can be rejected, and values $p < 0.0001$ indicate that the correlation is statistically significant at the 99.999 %-level

reduction was observed in the strongest brightening months during the brightening period, but based on the performance of the GWL models this cloud reduction cannot fully account for the total increase in atmospheric transmittance. The change in broadband aerosol optical depth in Bergen from around 0.15 before 1990 to around 0.10 in the 2000s, identified in Parding et al. (2014), may be a contribution factor to the observed brightening. The aerosol optical depth calculations in Parding et al. (2014) showed no significant change between 1965 and 1990, again suggesting that the observed dimming in Bergen is associated with large scale weather patterns rather than aerosols.

While the atmospheric transmittance is captured poorly by the empirical GWL model during the recent brightening period (after 1990), the relative sunshine duration is represented reasonably well during the same period. This apparent discrepancy may be due to the fact that global irradiance varies on a continuous scale while sunshine duration is a threshold measurement with only one of two values at each time: sunny or not sunny. Small and gradual changes in atmospheric turbidity (e.g., aerosol optical depth or cloud optical properties) can have a considerable influence on global irradiance without the direct irradiance falling into a different category with regards to the sunshine duration

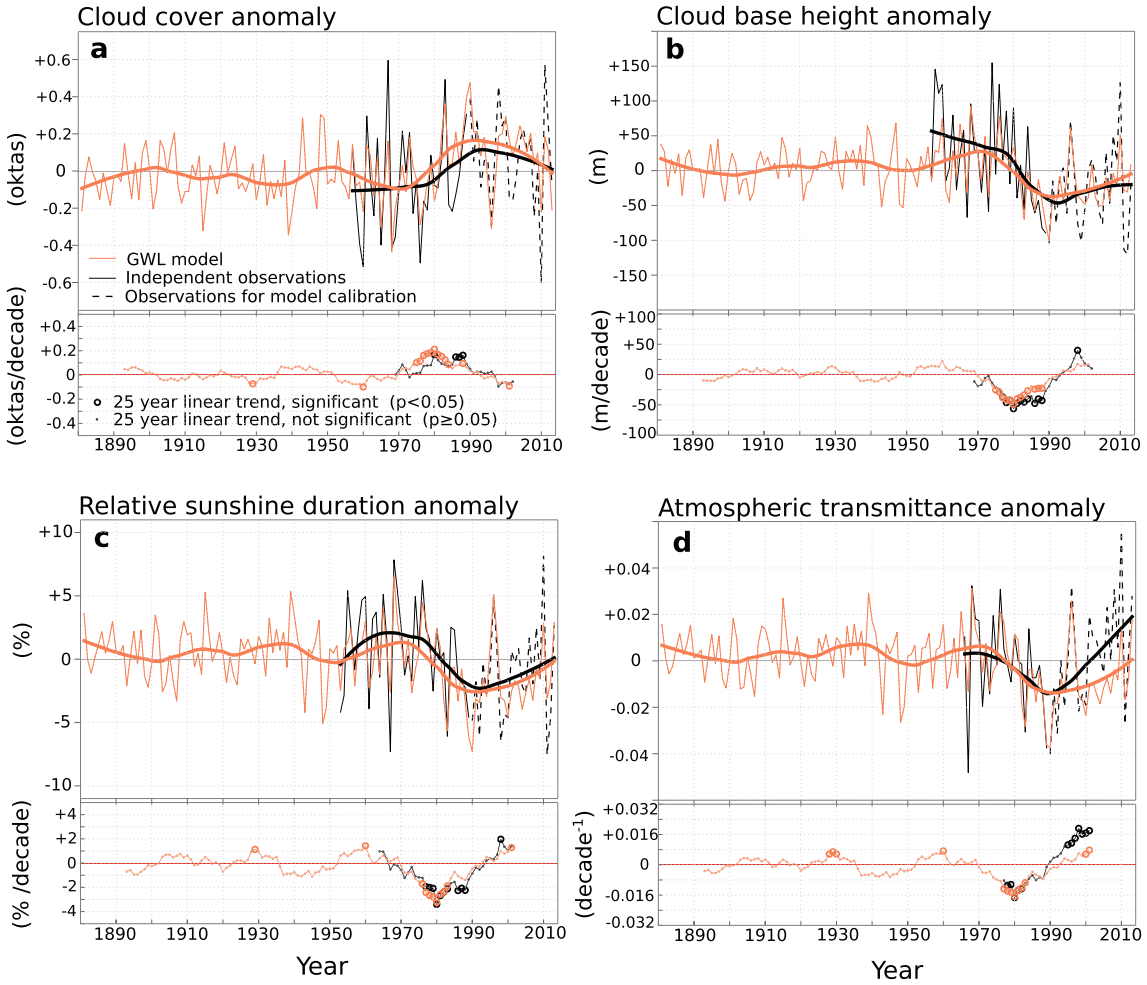

Fig. 3 Observational time series and simulations from Bergen, Norway of **a** cloud cover, **b** cloud base, **c** relative sunshine duration, and **d** atmospheric transmittance (normalised global irradiance) based on a daily weather pattern classification data set as described in Section 3, calibrated with observational data from 1990–2013. Two plots are included for each variable, the upper one showing the annual mean (*thin lines*) and smoothed (*thicker lines*, lower curves with a 40 year smoothing window) observational (*black*) and modeled (*orange*) time series. In the lower panel, the *markers* represent the slope of linear fits calculated for 25 year long periods with the abscissa representing the center of the time period (year±12 years). *Large circles* indicate that a trend is statistically significant at the 95 %-level, and *small dots* indicate that the trend is not statistically significant, as estimated by the Mann-Kendall test. Trend estimates are shown for both observational (*black markers*) and modeled (*orange markers*) time series

threshold. Hence, the difference between relative sunshine duration and atmospheric transmittance during the brightening period can be interpreted as further support of the influence of reduced aerosol emissions on the SW irradiance.

Because the model simulations of the cloud cover, cloud base, and relative sunshine duration agree well with the observations, both during the calibration period (1990–2013) and before (<1990), we assume that the extended model time series (1881–2013) is representative of past weather variability during the pre-observation period. The atmospheric transmittance model may also be representative of the portion of past SW irradiance variability that is associated with the large scale atmospheric circulation, but because of its sensitivity to other factors it may not capture past variations during periods of changing atmospheric turbidity. The model time series of relative sunshine duration and cloud cover are strongly anti-correlated ($R = -0.99$) and both indicate that the shift around 1981 is unprecedented during the 20th century (Fig. 3a, c). Figure 4 shows the model time series of relative sunshine duration and cloud cover, with markers indicating the top and bottom 10th percentile model values marked, i.e., the 14 highest and lowest years. Of the 14 most cloudy years, 10 occur after 1980, and of the 14 most sunny years, 11 are found before 1980. The cloud base and atmospheric transmittance models too show

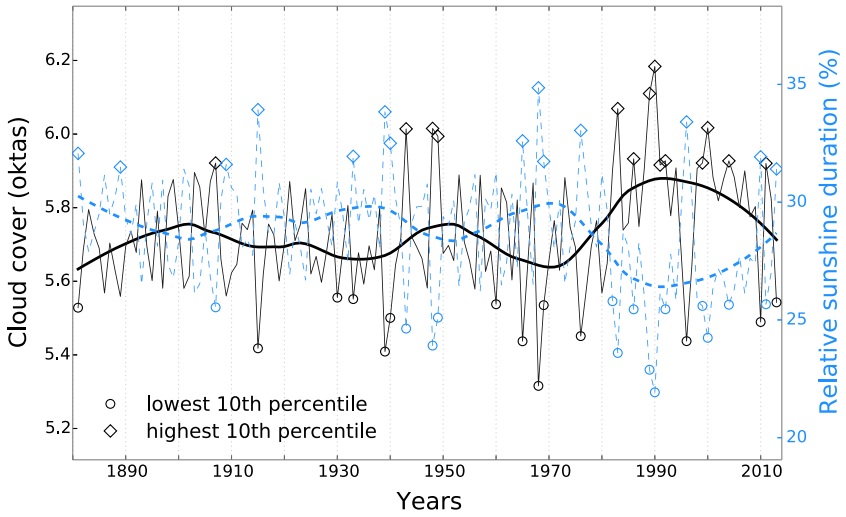

Fig. 4 Model simulations of cloud cover (*black solid lines*) and relative sunshine duration (*blue dashed lines*) based on GWL data as described in Section 3, calibrated with observational data from 1990–2013 for Bergen, Norway. The *thicker lines* are smoothed versions (lowest curves with a 40 year smoothing window) of the model time series which have a 1-year resolution. The highest and lowest 10th percentile values of modeled cloud cover and relative sunshine duration are marked in the figure. The model performance for the marked highest and lowest 10th percentile years are used to evaluate the importance of different weather patterns in Section 4.2

no significant trends from 1881 to the start of the dimming period (Fig. 3b, d).

4.2 Relationship between GWL and surface weather conditions

To investigate how cloud and solar conditions in Bergen are connected to certain large scale meteorological patterns, we study the individual components of the GWL models. Table 2 shows the model coefficients (c_i in Eq. 1) of the cloud cover, cloud base, relative sunshine duration, and atmospheric transmittance models for Bergen. Remember, model coefficients (c_i in Eq. 1) are a measure of the local solar and cloud anomalies associated with each of the 29 GWL, displayed in Fig. 1.

An immediately obvious feature of Table 2 is that weather patterns with positive coefficients in the cloud cover model have negative coefficients in the relative sunshine duration and atmospheric transmittance models and vice versa. This simply means that weather patterns associated with anomalously cloudy conditions are accompanied by reduced atmospheric transmittance and relative sunshine duration. The opposing cloud cover and solar coefficients support the hypothesis that the synoptic weather patterns act on the solar radiation primarily via the cloud cover.

The coefficients of the cloud base and cloud cover models also tend to be of opposite sign, i.e., for weather patterns associated with anomalously cloudy conditions, the clouds tend to have a lower base height than average. Low clouds tend to be optically thicker than their mid and high level counterparts so the presence of low cloud may also contribute to the reduced SW irradiance associated with the cloudy weather patterns (Olseth and Skartveit 1993).

The relationship between weather patterns and clouds appears to be connected to cyclonic and anti-cyclonic weather patterns, but the direction of the wind flow over the mountainous Norwegian coast likely also has an important influence on the cloudiness. The weather patterns that are associated with anomalously cloudy conditions (GWL 1, 2, 4–10, 16) are characterised by large scale low SLP systems centered over the North Atlantic, Norwegian Sea or Scandinavia, and, in many cases, a high SLP system over central and southern Europe (see Fig. 1 and Table 2). What the SLP maps indicate in these cases is essentially a storm track with westerly flow over Norway (Fig. 1). The increased cloudiness in Bergen can be explained by the combined effect of frontal zone clouds associated with cyclones and orographic lifting as the westerly flow meets the mountainous terrain (Houze 2014). Most of the anomalously sunny conditions in Bergen are associated with high SLP systems centered over Northern Europe (GWL 17–25) or the UK and Norwegian Sea (GWL 11–15). These situations are typically characterised by an easterly or north-easterly flow over Bergen. The reduced cloudiness makes sense in these cases as subsidence is expected in the vicinity of anti-cyclonic systems, but also because of the downslope wind that results from the easterly flow from mountains towards sea. The importance of the wind direction is further supported by the fact that GWL 3 is associated with more sunny conditions than usual in Bergen. This weather pattern is characterised by a cyclonic system over central Europe and easterly or south-

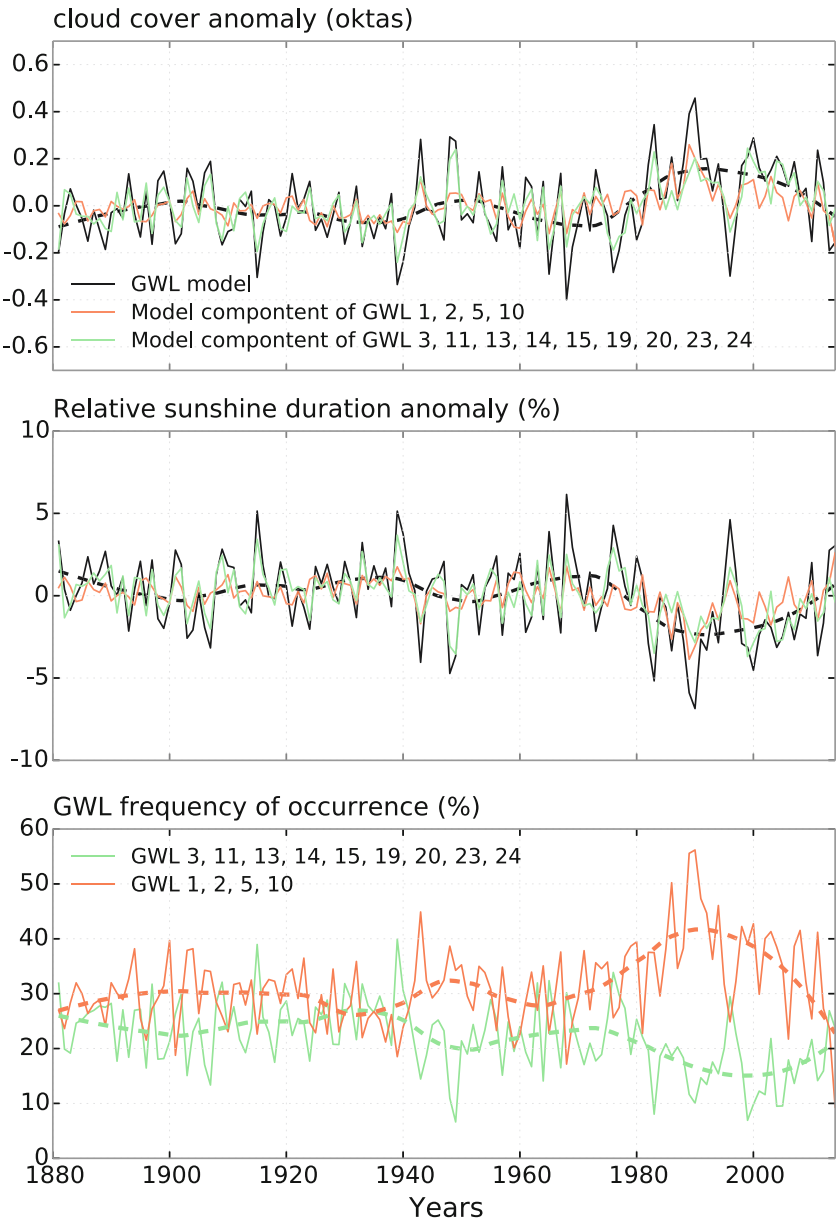

Fig. 5 The two upper panels show the components of the GWL models of cloud cover (**a**) and relative sunshine duration (**b**) associated with two groups of weather patterns: GWL (cloudy) = GWL 1, 2, 5, and 10 which are associated with cloudy conditions in Bergen and cyclonic systems centered over the North Atlantic and Northern Europe region, and GWL (sunny) = GWL 3, 11, 13, 14, 15, 19, 20, 23, which are associated with more sunny than average conditions in Bergen and anticyclonic systems over Scandinavia (GWL 19, 20, 23), the Norwegian Sea (GWL 11, 13, 14, 15), and/or easterly flow over Norway (GWL 3, 11, 13, 14, 15). The lower panel (**c**) shows the total frequency of occurrence of two groups, GWL (cloudy) and GWL (sunny)

easterly flow over Scandinavia. Based on the SLP pattern of GWL 3, the most likely explanation for the reduced cloudiness in Bergen is orographic subsidence as a result of the wind direction.

To identify the weather patterns that have had the strongest influence on local weather variability in Bergen, we study the top and bottom 10th percentile values of the cloud cover and relative sunshine models (Fig. 4). The contribution of the individual weather patterns to the top 10th percentile is estimated by multiplying the model coefficients (c_i), by the frequency anomaly of the GWL during the highest 14 years.

For example, the relative sunshine duration model has a coefficient +28 % for GWL 20 (Scandinavian high, ridge over central Europe), which shows that the weather pattern is associated with sunnier than average conditions in Bergen (Table 2). The average frequency of occurrence of GWL 20 is only 3.5 % from 1881 to 2013 but 5.5 % during the most sunny years. The net effect of the above-mentioned frequency increase on the relative sunshine duration is estimated as 28 % × 0.02 = +0.56 %. This may seem like a modest contribution, but GWL 20 accounts for more than one-eighth of the average relative sunshine duration anomaly in the top 10th percentile.

Frequency changes of weather patterns associated with cloudy conditions can also have a substantial contribution in sunny years. For example, GWL 2 (cyclonic westerly flow over central and northern Europe) has a model coefficient of −10 % for the relative sunshine duration. GWL 2 is the most commonly occurring weather pattern with an

Table 2 Coefficients of the empirical GWL models of cloud cover (NN), cloud base (HL), relative sunshine duration (RSD), and atmospheric transmittance (Tr) for Bergen, Norway

c_i	NN (oktas)	HL (m)	RSD (%)	Tr
c_1	*+1.1*	−311	−16	−0.10
c_2	*+0.6*	−184	−10	−0.05
c_3	−0.9	*+339*	*+6*	*+0.01*
c_4	*+0.4*	*+166*	−9	−0.08
c_5	*+1.1*	−273	−17	−0.13
c_6	*+0.4*	−116	−6	−0.03
c_7	*+0.6*	−266	−9	−0.05
c_8	*+0.2*	−174	−2	−0.0
c_9	*+0.5*	−26	−6	−0.05
c_{10}	*+0.9*	−212	−11	−0.06
c_{11}	−1.1	*+298*	*+22*	*+0.14*
c_{12}	−1.3	*+122*	*+24*	*+0.13*
c_{13}	−1.3	*+102*	*+22*	*+0.12*
c_{14}	−1.4	*+232*	*+22*	*+0.14*
c_{15}	−2.0	*+322*	*+28*	*+0.18*
c_{16}	*+0.2*	−108	*+1*	*+0.01*
c_{17}	−0.6	*+92*	*+8*	*+0.06*
c_{18}	−1.1	*+215*	*+19*	*+0.12*
c_{19}	−1.4	*+395*	*+21*	*+0.13*
c_{20}	−1.8	*+593*	*+28*	*+0.13*
c_{21}	−1.5	*+524*	*+22*	*+0.10*
c_{22}	−2.7	*+744*	*+41*	*+0.23*
c_{23}	−2.4	*+708*	*+36*	*+0.18*
c_{24}	−1.1	*+516*	*+16*	*+0.05*
c_{25}	−0.4	*+318*	*+4*	*+0.03*
c_{26}	*+0.3*	*+66*	−3	−0.04
c_{27}	*+0.3*	*+104*	−8	−0.05
c_{28}	−0.4	*+153*	*+10*	*+0.08*
c_{29}	−0	*+52*	*+1*	*+0.02*

The coefficients represent local solar and cloud anomalies associated with the GWL weather patterns (see Section 3). Positive c_i are marked with italic font to facilitate identifying patterns among model coefficients, e.g., that GWL with positive NN coefficients tend to have negative RSD and Tr coefficients, and vice versa

average frequency of 15.5 % from 1881 to 2013. During the 14 sunniest years, the average frequency of GWL 2 is reduced to 11.5 %, which contributes $(-10\,\%) \times (-0.04) = +0.4\,\%$ to the relative sunshine duration peaks in Bergen.

Similarly, the 14 least sunny years (lowest 10th percentile) can be traced to a decrease in the frequency of GWL associated with sunny conditions (relative sunshine duration coefficients $c_i > 0$) such as GWL 20, and increasing occurrence of weather patterns associated with negative sunshine anomalies ($c_i < 0$), like GWL 2.

After quantifying the contribution of the individual GWL to cloud cover and relative sunshine duration models in peak years as described above, we identify the top 12 contributing weather patterns, which together explain more than 85 % of the total variability of the model simulated cloud cover and relative sunshine duration. This analysis shows that some of the weather patterns that have a strong influence on the weather conditions in Bergen when they occur, e.g., GWL 21 and 22 (see Table 2), do not contribute much to the empirical models because they occur so seldom. The selected weather patterns can be divided into two groups based on their observed influence on Bergen.

GWL (cloudy) GWL 1, 2, 5, and 10 are associated with anomalously cloudy conditions and reduced relative sunshine duration (Table 2). They are characterised by low SLP over the Norwegian Sea, high SLP over central or southern Europe (Fig. 1), and a westerly flow from the ocean towards the west coast of Norway.

GWL (sunny) GWL 3, 11, 13, 14, 15, 19, 20, and 23, are associated with anomalously sunny and cloud free conditions in Bergen. Many of these weather patterns are indicative of blocking situations over Scandinavia (GWL 19, 20, 23) or Iceland (GWL 14, 15) and have been used as such in an early study of blocking action in the European region by Brezowsky et al. (1951). Some of the GWL (sunny) weather patterns also have SLP patterns that indicate a south-easterly to north-easterly flow from the inland towards the Norwegian coast (GWL 3, 11, 13, 14, 15). Orographic subsidence may be an important factor in the reduced cloudiness connected to these weather patterns.

4.3 Decadal variability of the Grosswetterlagen and their influence on the weather conditions in Bergen

The changes of clouds and sunshine observed in Bergen (see Parding et al. 2014) can be traced to the varying frequency of the two groups of weather patterns identified above. Figure 5 shows the frequency variations of GWL (cloudy)—characterised by cyclonic and westerly flow over northern Europe—and GWL (sunny)—mostly Scandinavian blocking situations and easterly flow over the region—and their contributions to the GWL models of cloud cover and relative sunshine duration.

The total frequency of GWL (cloudy) is relatively stable before the shift around 1980/1981, occurring on average 30 % during the period 1881–1980. The GWL (sunny) weather patterns are more rare, with an average total frequency of 22 % during the same period. During the observed dimming in Bergen, the occurrence of the cyclonic GWL(cloudy) patterns increase and GWL (sunny) weather

patterns become more rare. After 1980, the total frequency of the GWL (cloudy) is 37 % while GWL (sunny) occur only 15 % of the days.

Together, the shifts in GWL (cloudy) and GWL (sunny) fully account for the observed and modeled trends in cloud cover and relative sunshine duration (Fig. 5). The increasing (decreasing) cloud cover (relative sunshine duration) in the late 1970s and 1980s can be connected to an increasing frequency of GWL (cloudy) and a decreasing frequency of GWL (sunny) weather patterns. Based on change point analysis as described in Lund and Reeves (2002), the increasing frequency of GWL (cloudy) may be described as a sudden shift in the mid 1980s. The frequency of the GWL (sunny) weather patterns is better characterised as a gradual and significant negative trend. However, looking specifically at the Scandinavian blocking patterns (GWL 19, 20, 23) reveals a significant and sudden drop of −3 percentage points around 1980 (not shown visually). The change point analysis alone could be interpreted as a sign of inhomogeneities in the GWL data set, but the connection between the GWL shifts and the observed changes in the meteorological conditions in Bergen indicate that the change points represent a shift in the climate regime of the region.

The temporal variations of the GWL (cloudy) and GWL (sunny) weather patterns largely mirror each other, the GWL (cloudy) increasing in frequency when GWL (sunny) become less frequent and vice versa (Fig. 5c). There is a moderate but significant anticorrelation ($R = -0.55$) between the annual mean frequencies of GWL (sunny) and GWL (cloudy), and a stronger negative correlation when considering smoothed time series ($R = -0.81$ for the 10 year moving average, not shown visually). In other words, the varying frequency of cyclonic and anticyclonic weather patterns in the north Atlantic and Scandinavian region are not independent but can be thought of as two expressions of the same development.

4.4 Relationship between the Grosswetterlagen and the North Atlantic Oscillation/Arctic Oscillation

The variations of atmospheric circulation described by way of the GWL can also be understood in terms of well-known climate indices. Here, we investigate two circulation patterns, the Arctic Ocillation (AO) and North AO (NAO), which are closely related and both have been identified as important contributions to the climate variability in the European and North Atlantic region (Budikova 2012; Hurrell 1995; Thompson and Wallace 1998; Jones et al. 1997). There is a positive correlation between the AO and NAO index and strong similarities between the SLP patterns and influence on weather conditions associated with the two climate oscillations. The NAO is sometimes described as a local expression of the AO, but others argue that the NAO and AO represent separate processes or perspectives of the Arctic climate (Ambaum 2001).

The AO, also referred to as the Northern annual mode (NAM), is a general pattern of the atmospheric pressure difference between the Arctic and northern hemisphere midlatitudes around 45° N (Budikova 2012). The AO index is usually calculated as the leading empirical orthogonal function (EOF) of the sea level pressure north of 20° N (Thompson and Wallace 1998, 2000). The NAO is a measure of the North-South pressure gradient specifically in the North Atlantic region, calculated as the normalised difference between the SLP measured at Iceland and the Azores (Hurrell 1995; Hurrell and Deser 2009; Jones et al. 1997; Xu and Jinqing 2013). Here, we use a principal component-based NAO index obtained by EOF analysis of the monthly SLP anomalies over the Atlantic sector (20–80 N, 90 W–40 E), retrieved from the UCAR/NCAR Climate Data Guide.

The AO and NAO are primarily winter features and do not represent the dominant circulation pattern as clearly in the summer half-year. For the principle component-based AO and NAO indices that we use here, the loading patterns are dominated by the cold season because the pressure variability is the strongest during this time of year. The comparison between the climate indices and the GWL are therefore restricted to the extended winter season, December–March.

During the positive phase of the AO (AO(+)), the SLP in the Arctic is anomalously low and the SLP in midlatitudes anomalously high. AO(+) is indicative of a strengthened polar vortex, a strong zonal upper level flow that locks in the Arctic cold air masses, and hinder exchange with midlatitudes. The often concurrent AO(+) and NAO(+) are both associated with warmer and moister winters than usual in northern Europe and increased frequencies of storms in this region.

The negative phase (AO(−)) is characterised by a reduced pressure gradient (higher than normal atmospheric pressure in the Arctic region and lower pressure over the midlatitudes), reduced strength of upper level winds, and a more meridional hemispheric flow which allows for intrusions of Arctic air farther south than usual (Budikova 2012). The jet stream and storm tracks shift southward during the AO(−) phase and in northern European winter, periods of AO(−) and NAO(−) which often overlap are associated with cold, dry, and sunny conditions.

The winter signature of the AO and NAO can be seen in the GWL data set as an increased frequency of GWL (cloudy) weather patterns during the AO(+) and NAO(+) phase (Fig. 6), which can be interpreted as an increase of the storm frequency over northern Europe. The frequency of many of the GWL (sunny) weather patterns are reduced in AO(+) and NAO(+) situations. This indicates that the positive phase of the NAO and AO is associated with reduced blocking action over Scandinavia and the Norwegian Sea.

The tendency is opposite during the AO(−) and NAO(−) phase: the GWL (cloudy) patterns are reduced in frequency while the GWL (sunny) weather patterns occur more often than average (Fig. 6).

The empirical model of the cloud cover for the extended winter period have a striking resemblance to the NAO and AO indices (Fig. 7). During the 1987/1988 shift from a negative to positive NAO/AO (de Laat and Crok 2013; Alheit et al. 1980), there is a sudden and significant shift in the winter cloud cover. The shift in the model simulated cloud cover and relative sunshine duration comes later in the winter season than when considering the annual mean time series. The AO/NAO and GWL can be used as complementary perspectives of the same circulation shift, the GWL providing a detailed and exact link between the local cloud and solar conditions and large scale circulation in Europe and the North Atlantic, and the NAO/AO putting the shift into a hemispheric context. The limitations of the climate indices is that they are representative for the cold season more than the summer. The strongest decadal changes in cloud cover and sunshine duration in Bergen occur in spring and late summer (Parding et al. 2014). Therefore, the GWL classification, which unlike the NAO/AO is well defined for all days of the year, is better suited to study the link between large scale weather patterns and local meteorological changes in this location.

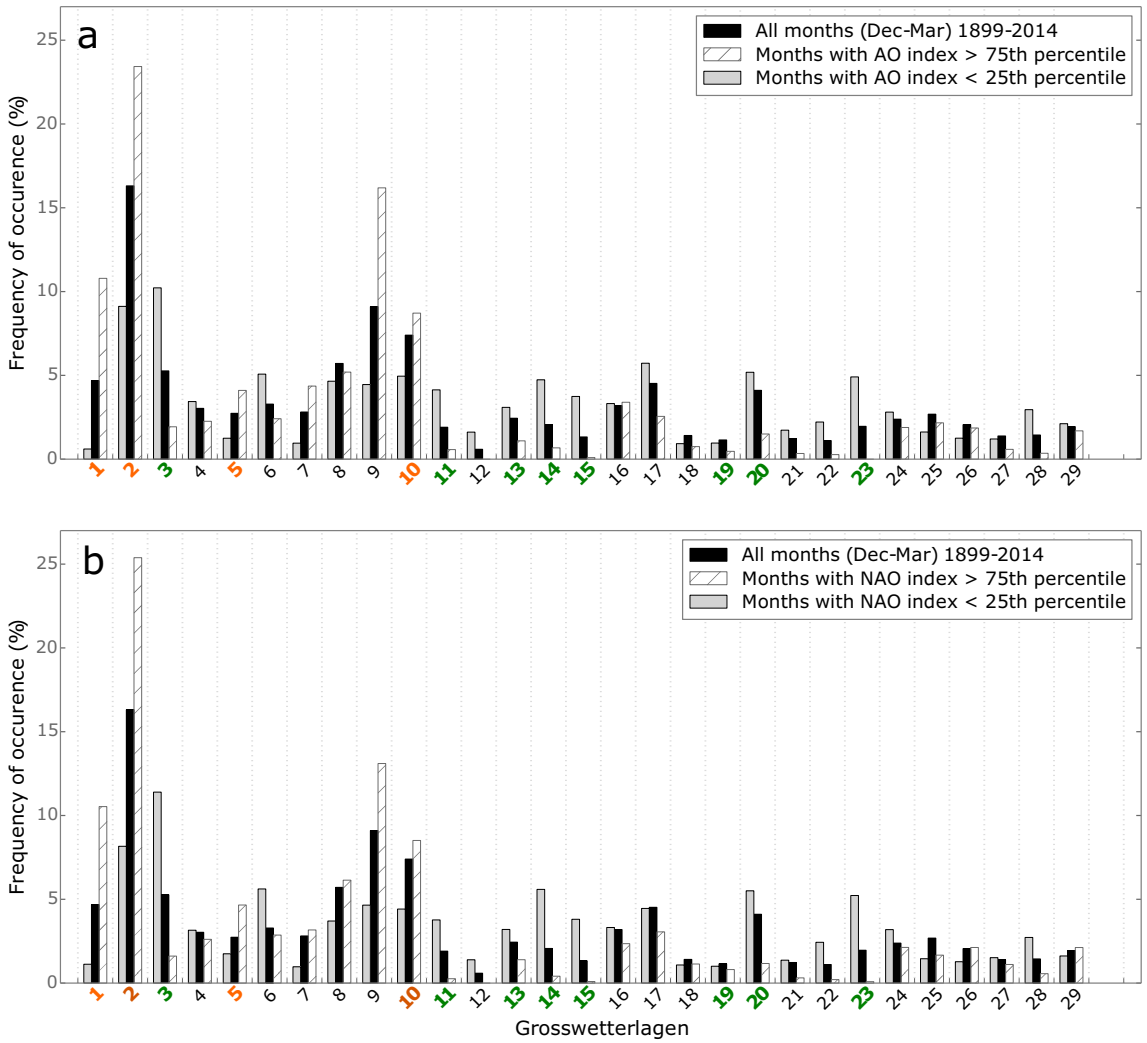

Fig. 6 Frequency of occurrence of the 29 Grosswetterlagen (GWL) large scale weather patterns over Europe and the North Atlantic for all months (*black*) as well as during the positive (*striped*) and negative (*grey*) phase of the Arctic Oscillation (AO) in the upper panel (**a**) and the North Atlantic Oscillation (NAO) in the lower panel (**b**). The GWL frequency is calculated based on all years of overlapping data of the climate index and GWL time series, 1899–2014 for the AO and 1881–2014 for the NAO. The positive and negative phase of the climate indices are defined here as the highest and lowest 25th percentiles. The bold colored GWL numbers mark two groups of weather patterns that have a strong influence on the solar and cloud conditions in Bergen (see Fig. 5)

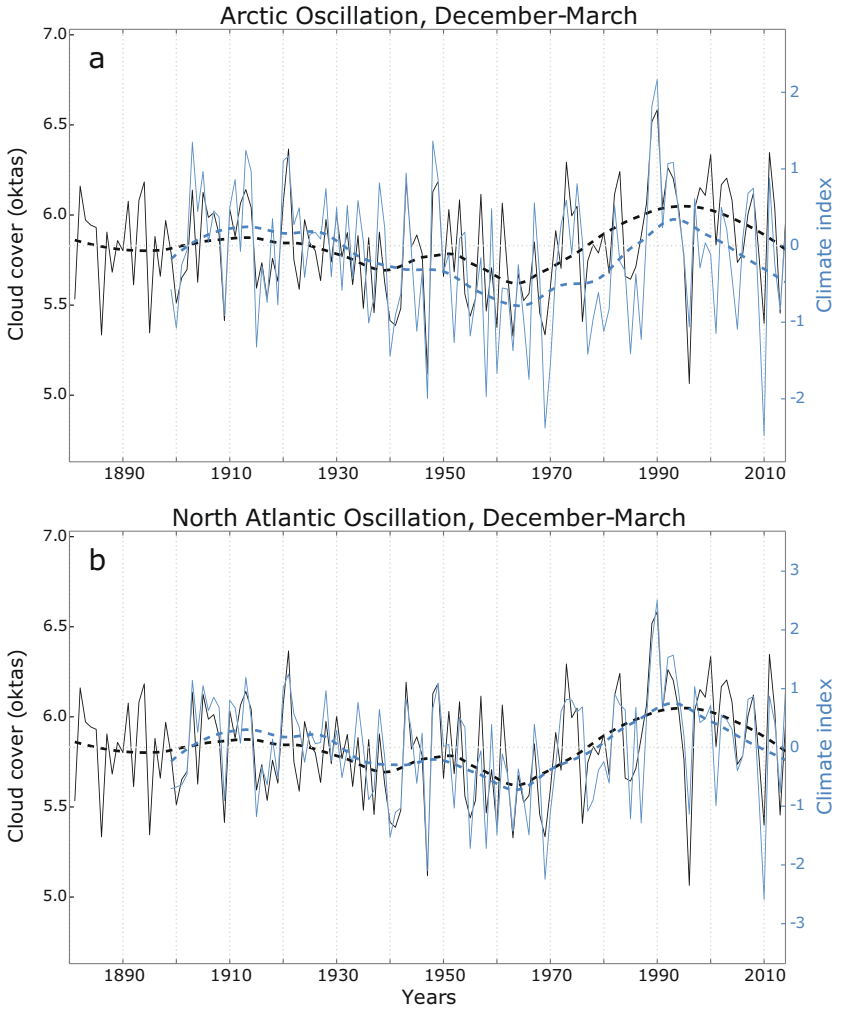

Fig. 7 Time series of the Arctic Oscillation (*blue lines*) and a reconstruction of cloud cover (*black line*) in Bergen generated by the empirical GWL (weather pattern) model as described in Section 3. The cloud cover model is compared against observed cloud cover in Section 4.1. The thin solid lines show the annual mean time series while the *dashed thicker lines* are lowest curves with a 40 year smoothing window

4.5 Summary and conclusions

Observational records from Bergen show an increase of the cloud cover and reduction of the cloud base during the late 1970s and 1980s, which is accompanied by a decrease of global irradiance and sunshine duration, i.e., a solar dimming. After 1990, there is an increase in normalised global irradiance which can be described as a brightening period, although it is not accompanied by decreasing cloud cover strong enough to account for the irradiance change. The brightening may be connected to a decrease in AOD (Parding et al. 2014). In a previous detailed study of the cloud and solar variability in Bergen, we (Parding et al. 2014) suggested that the dimming period was related to changes in the frequency of cloudy situations, in particular low clouds, associated with large scale weather patterns.

Here, we address the relationship between local and large scale weather by using the frequencies of GWL, a subjective classification of synoptic weather patterns in Europe from 1881 to 2013. Based on the GWL, we construct empirical linear models of cloud cover, cloud base, relative sunshine duration, and normalised global irradiance (atmospheric transmittance). The model coefficients are trained using daily observations of the cloud and solar variables from the calibration period 1990–2013 and tested with the remaining time series. The GWL models enables extending the observational cloud and solar time series by more than 70 years, back to 1881.

The GWL models successfully reproduce the observed cloud and solar changes during the dimming period in the late 1970s and 1980s. Change point analysis of the model simulated time series indicates that the change can be described as a sudden shift around 1980/1981. We interpret the good agreement between model simulations and independent observations as a strong indication that the dimming is related to shifts in the large scale atmospheric circulation. However, the recent observed brightening is not represented by the GWL models, suggesting that the recent increase of SW irradiance is associated with factors other than large scale atmospheric circulation. In Parding et al. (2014), we identify both seasonally varying changes in cloud cover and aerosols as likely contributions to the brightening in Bergen. The GWL model reproduces the observed atmospheric transmittance better

during the independent period (before 1990) than during the calibration period (1990–2013) which demonstrates that the modeling method works even when large scale weather patterns are not the dominant influence on local cloud and solar conditions.

A closer examination of the GWL models shows that the observed cloud and solar changes can be traced to an increased frequency of cyclonic weather patterns (GWL 1, 2, 5, 10) and a decreased frequency of weather patterns characterised by anticyclones over Scandinavia (GWL 19, 20, 23) and Iceland (GWL 14, 15) or other situations with easterly flow over Norway (GWL 3, 11, 13). The changing circulation patterns can also be understood in terms of a shift from the negative to the positive phase of the NAO and AO. However, the AO and NAO indices are limited to the winter while the GWL provides a valid description of the daily synoptic situation throughout the year, which is more relevant for our solar irradiance and sunshine duration investigation.

The atmospheric circulation changes described above do not necessarily have the same effect elsewhere in Europe. It is plausible that the circulation shifts have similar effects across larger parts of northern Europe than Bergen, but given the topography along the Norwegian coast and its influence on the cloud cover, the weather patterns may have a different result at inland sites. This subject is explored in a followup study where we specifically address the connection between large scale weather patterns and the observed dimming and brightening in northern Europe.

References

Alheit J, Mollmann C, Dutz J, Kornilovs G, Loewe P, Mohrholz V, Wasmund N (1980) Synchronous ecological regime shifts in the central Baltic and the North Sea in the late. ICES J Mar Sci 62:1205–1215

Ambaum M (2001) Arctic oscillation or North Atlantic oscillation? J Clim 14:3495–3507

Baur F, Hess P, Nagel H (1944) Kalender der Großwetterlagen Europas 1881–1939. Tech. rep., Forschungsinstitut für langfristige Wettervorhersage, Bad Homburg

Brezowsky H, Flohn H, Hess P (1951) Some remarks on the climatology of blocking action. Tellus (1949)

Budikova D (2012) Northern hemisphere climate variability: character, forcing mechanisms, and significance of the North Atlantic/Arctic Oscillation. Geogr Compass 7:401–422

Chiacchio M, Ewen T, Wild M, Arabini E (2010) Influence of climate shifts on decadal variations of surface solar radiation in Alaska. J Geophys Res 115:D00D21. doi:10.1029/2009JD012533

de Laat ATJ, Crok M (2013) A late 20th Century European climate shift: fingerprint of regional brightening? J Atmos Clim Sci 3:291–300

Gilgen H, Roesch A, Wild M, Ohmura A (2009) Decadal changes in shortwave irradiance at the surface in the period from 1960 to 2000 estimated from Global Energy Balance Archive Data. J Geophys Res 114:D00D08. doi:10.1029/2008JD011383

Hanssen-Bauer I (1967) A simple model for diffusion of SO2 in Bergen. Atmos Environ 19(3):415–422. doi:10.1016/0004-6981(85)90163-5

Houze R (2014) Chapter 12. Clouds and precipitation associated with hills and mountains. In: Cloud dynamics, 2nd edn. Academic Press, Elsevier, Amsterdam

Hurrell JW (1995) Decadal trends in the North Atlantic oscillation: regional temperatures and precipitation. Science 269:676–679

Hurrell JW, Deser C (2009) North Atlantic climate variability: the role of the North Atlantic Oscillation. J Mar Syst 78(1):28–41

Iqbal M (1983) An introduction to solar radiation, 1st edn. Academic Press Canada, Ontario

Jones PD, Jonsson T, Wheeler D (1997) Extension to the North Atlantic Oscillation using early instrumental pressure observations from Gibraltar and South-West Iceland. Int J Climatol 17:1433–1450

Kanamitsu M, Ebisuzaki W, Woollen J, Yang SK, Hnilo JJ, Fiorino M, Potter GL (2002) NCEP-DOE AMIP-II Reanalysis (R-2). Bulletin of the American Meteorological Society, pp 1631–1643

Kopp G, Lean JL (2011) A new, lower value of total solar irradiance: evidence and climate significance. Geophys Res Lett 38(1), L01706. doi:10.1029/2010GL045777

Liepert BG (2002) Observed reductions of surface solar radiation at sites in the United States and worldwide from 1961 to 1990. Geophys Res Lett 29(10):1421. doi:10.1029/2002GL014910

Liley JB (2009) New Zealand dimming and brightening. J Geophys Res 114:D00D10. doi:10.1029/2008JD011401

Lund R, Reeves J (2002) Detection of undocumented changepoints: a revision of the two-phase regression model. J Clim 15:2547–2554

Olseth JA, Skartveit A (1993) Characteristics of hourly global irradiance modelled from cloud data. Solar Energy 51(3):197–204

Parding K, Olseth JA, Dagestad KF, Liepert BG (2014) Decadal variability of clouds, solar radiation and temperature at a high-latitude coastal site in Norway. Tellus B 66:25897. doi:10.3402/tellusb.v66.25897

Russak V (2009) Changes in solar radiation and their influence on temperature trend in Estonia (1955–2007). J Geophys Res 114:D00D01. doi:10.1029/2008JD010613

Stanhill G (2003) Through a glass brightly: some new light on the Campbell Stokes sunshine recorder. Weather 58 January

Stanhill G, Cohen S (2001) Global dimming: a review of the evidence for a widespread and significant reduction in global radiation with discussion of its probable causes and possible agricultural consequences. Agric For Meteorol 107(4):255–278

Stjern CW, Kristjánsson JE, Hansen AW (2009) Global dimming and global brightening—an analysis of surface radiation and cloud cover data in northern Europe. Int J Climatol 29:643–653

Thompson DWJ, Wallace JM (1998) The Arctic Oscillation signature in the wintertime geopotential height and temperature field. Geophys Res Lett 25(9):1297–1300

Thompson DWJ, Wallace JM (2000) Annular mode in the extratropical circulation. Part I: month-to-month variability. J Clim 13:1000–1016

Werner PC, Gerstengarbe FW (2010) Katalog der Großwetterlagen Europas (1881–2009) nach Paul Hess und Helmut Brezowsky, 7. verbesserte und ergänzte Auflage. PIK report 119

Wild M (2012) Enlightening global dimming and brightening. Bull Am Meteorol Soc 93(1):27–37. doi:10.1175/BAMS-D-11-00074.1

Wild M, Gilgen H, Roesch A, Ohmura A, Long CN, Dutton EG, Forgan B, Kallis A, Russak V, Tsvetkov A (2005) From dimming to brightening: decadal changes in solar radiation at Earth's surface. Science (New York NY) 308(5723):847–850. doi:10.1126/science.1103215. http://www.ncbi.nlm.nih.gov/pubmed/15879214

WMO (2008) Observations of clouds. In: WMO guide to meteorological instruments and methods of observations. Part I. Measurements of meteorological variables, chap 15

Xu L, Jinqing ZUO (2013) Impact of the North Atlantic Sea surface temperature tripole on the East Asian Summer Monsoon. Adv Atmos Sci 30(4):1173–1186. doi:10.1007/s00376-012-2125-5